

2008

Experimental and Computational Study of Area and Perimeter Contributions to Radiometer Forces

N P. Selden

University of Southern California, Los Angeles, California

S F. Gimelshein

ERC, Inc.

E P. Muntz

University of Southern California, Los Angeles, California

Alina A. Alexeenko

Purdue University - Main Campus, alexeenk@purdue.edu

A D. Ketsdever

University of Colorado

Follow this and additional works at: <http://docs.lib.purdue.edu/aaepubs>



Part of the [Engineering Commons](#)

Recommended Citation

Selden, N P.; Gimelshein, S F.; Muntz, E P.; Alexeenko, Alina A.; and Ketsdever, A D., "Experimental and Computational Study of Area and Perimeter Contributions to Radiometer Forces" (2008). *School of Aeronautics and Astronautics Faculty Publications*. Paper 20.
<http://dx.doi.org/10.1063/1.3076616>

This document has been made available through Purdue e-Pubs, a service of the Purdue University Libraries. Please contact epubs@purdue.edu for additional information.

Experimental and Computational Study of Area and Perimeter Contributions to Radiometer Forces

N.P. Selden^a, S.F. Gimelshein^b, E.P. Muntz^a, A. Alexeenko^c, and A.D. Ketsdever^d

^aUniversity of Southern California, Los Angeles, CA 90089

^bERC, Inc., Edwards AFB, CA 93528

^cPurdue University, West Lafayette, IN 47907

^dUniversity of Colorado, Colorado Springs, CO 80933

Abstract. The relative contribution to the radiometric force of the area and perimeter of the vane is studied experimentally and numerically. Experimentally, a circular vane, a low-aspect rectangular vane, and a high-aspect rectangular vane were all tested on a force balance, with nano-Newton resolution, placed in a stagnant gas. The computational results were obtained through 2-D simulations using the direct simulation Monte Carlo method, as well as a discrete ordinate solution of the ES model kinetic equation. Gas pressure was varied from 0.006 to 6 Pa, which was a broad enough range to observe the characteristic peak force production of a radiometer in the transition regime, where the peak occurs at $Kn \sim 0.1$. It was found that the area of a radiometer vane is responsible for a significant amount of the total force production through a wide range of operating pressures. It is only at the highest background pressures, well after force production has peaked, that the vane perimeter appears to dominate the operation of the radiometer.

Keywords: Radiometric force, area and perimeter contributions, thrust stand, kinetic modeling.

PACS: 51.10.+y

INTRODUCTION

The objective of this work is to compare experimentally measured forces created by rarefied gas flows on heated plates of different shapes and numerical simulations of the total force as a function of gas pressure. The foundation for this work was laid in the distant past by William Crookes^{1,2} who invented the radiometer in the 1870's. It was his novel apparatus, and his pioneering work, which helped develop and validate the fledgling branch of science now known as gas kinetics. Simply designed, it consisted of an airtight bulb under partial vacuum with a series of half-blackened vanes mounted on a spindle. When light was shone on the device, the vanes began to rotate on the spindle with the half-blackened sides retreating from the light source. Though Crookes initially believed he was directly measuring photon pressure, a series of investigations by other prominent scientists of the era proved something entirely different was responsible.

Reynolds first suggested that the force was due to surface outgassing, and then presented a more rigorous explanation based on kinetic theory.³ According to the latter theory, the gas in the partially evacuated bulb is the main driving force responsible for the rotation of the vanes. Further work was done by Schuster⁴ which turned up the first experimental evidence of gas forces being the dominant cause of the radiometric effect. The kinetic theory explanation is in fact a free molecule approximation of the radiometric effect: after the light heats the blackened side of the vane, the molecules reflect from the hot side with higher average velocities. This leads to a larger momentum imparted to the hot side, and results in the motion of the vanes with the hot side trailing.

Reynolds also proposed that increasing the pressure in the bulb would dramatically affect the device's operation. He theorized that the onset of intermolecular collisions in the gas would work to equalize the pressure on both sides of the vane, and under sufficiently high pressures (near-continuum) the force production would drop rapidly.⁵ With further exploration, Maxwell⁶ showed that an unbalanced force exists near the edge of the heated side of the vane, where the heat flow in the gas is non-uniform. Though a unique result for the time, it took another fifty years before Einstein presented a simple theory⁷ that related the force on the vanes to their perimeter. This edge dependence of

the vane force has found partial confirmation in experimental work⁸ where the force was found to depend on perimeter. Although the dependence was not shown to behave exactly as Einstein had predicted, the edge theory of the radiometer has become widely accepted.

It was with this understanding that interest in the radiometer problem declined steadily after 1928, mostly because the issue of force production was considered closed, and no direct application for radiometric forces had been identified at that time. The phenomenon that drives Crookes' radiometer has been summarized by Draper⁹ who in effect described our present understanding of it: a temperature gradient along a surface creates tangential stresses in the gas, and as a result the gas moves over the surface from the cold to the hot side. For the gas to be accelerated in this manner, it is required that an equal and opposite force propel the plate in the opposite direction. Under this explanation, the main contribution of the force to the rotation of the vanes comes from the an area very near the edge (a zone with a width of a mean free path λ , according to Einstein).

Lack of an obvious application may explain the miniscule interest in the problem in the second half of the last century, when only a few research papers on the subject were published¹⁰ with other publications being historic analyses and overviews. The situation has changed over the last decade, as the radiometric phenomenon has been found to have possible uses in a number of different micro- and macro-scale devices. The forces produced by temperature gradients in a gas have been shown¹¹ to be applicable to modern microactuator, where the direct simulation Monte Carlo (DSMC) method was used to model forces on vanes mounted on an armature. This method, along with experimental measurements, has been employed¹² to study a concept of an opto-microengine that uses radiometric forces. Subsequently, a series of papers by Passian with co-workers was published,^{13,14} where radiometric phenomena were studied experimentally and analytically, mostly with application to microcantilevers. The use of radiometric forces as an approach to study gas-surface translational energy accommodation has also been mentioned by Passian et al in a third paper,¹⁵ and a new concept of a high-altitude aircraft supported by microwave energy that uses radiometric effects was put forward by Benford.¹⁶

The new studies of the old radiometric phenomena have been supported on the one hand by modern technologies that allow more accurate measurements, and on the other hand by state-of-the-art numerical methods that rely heavily on parallel computing. These two factors, along with the revived interest in the application of radiometric phenomena, have prompted the authors to revisit the contribution of the “collisionless” (area) versus the “collisional” (edge) forces to the total radiometric force.

EXPERIMENTAL SETUP

To study the role of area and edge forces on the plate, three radiometer vane geometries were used. Each of these consisted of a Teflon insulator sandwiched between two aluminum plates. A resistive heater was located between one of the plates and the Teflon insulator, and the temperature of the hot side of the device was maintained by varying the power input to the heater. Each of the plates and insulator are 0.32cm thick, and when assembled yield a total device thickness of 0.95cm. Figure 1 shows a schematic of one of the devices used for both experimental and computational comparisons. The first device was a rectangle 3.81 x 12.7cm, the second device was a rectangle with exactly double the area having dimensions of 7.62 x 12.7cm, and the third was a circle with a diameter of 11.13cm and an area equivalent to that of the large rectangle.

Each of these devices was individually mounted on a modified nano-Newton Thrust Stand (nNTS)¹⁷ located inside of a 0.4m diameter vacuum chamber. When calibrated using a set of electrostatic combs,¹⁸ the nNTS provides very accurate and repeatable data with typical force resolution of approximately 0.1 μ N and statistical scatter around 1%. The experimental error based on standard deviation ranges from a few percent at the lowest pressures to approximately 1% through most of the curve. However, due to the normalization by experimental temperature measurements, the variation in background pressure, and the small uncertainty of the calibration method, the total absolute experimental uncertainty is approximately 4%. Day-to-day variation of multiple data sets has been observed to be about 2%.

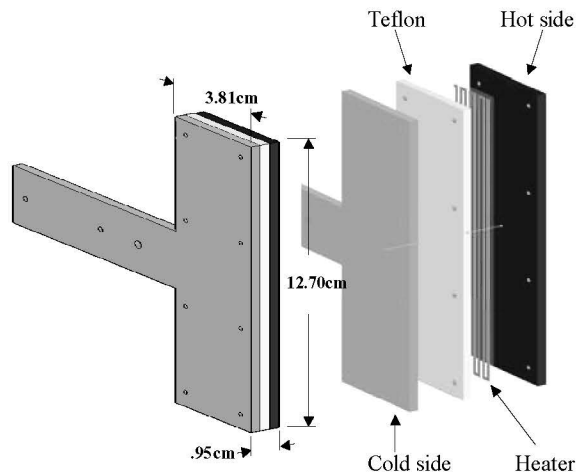


FIGURE 1. Schematic of a radiometric device.

The experimental data was obtained for each device by evacuating the chamber to a base pressure below 10^{-3} Pa. A constant voltage was applied to the heater, and this resulted in the main surfaces reaching temperatures of approximately 415K (hot) and 365K (cold). The background pressure inside the chamber was varied by flooding the chamber with a specific gas over a range of pressures from 0.02Pa to 1.4Pa. Argon, helium, and nitrogen were all utilized with the additional use of xenon.

The experimentally measured force was normalized by the temperature difference between the hot and cold plates, ΔT , for the purpose of comparing results for different pressures and gases. Verification of the validity of the experimental normalization method is demonstrated in a prior paper¹⁹ where exceptional linearity with temperature difference is observed.

COMPUTATIONAL SETUP

Two kinetic approaches were used in the work, the direct simulation Monte Carlo (DSMC) method and a finite difference solution of the ellipsoidal statistical (ES) model kinetic equation. The DSMC computational tool, SMILE²⁰ was used in all DSMC computations presented in this work. The variable hard sphere model²¹ was used for the intermolecular potential, and the Larsen-Borgnakke model with variable rotational relaxation number used for translational-internal energy transfer. The gas-surface model was assumed to be diffuse with full energy accommodation. A two-dimensional module of SMILE was used in this work because three-dimensional modeling is prohibitively expensive for most pressures under consideration. The computations were conducted for two plates with dimensions 0.95x3.81cm and 0.95x7.62cm immersed in an initially uniform stagnant gas in a chamber. The third (Z-axis) dimension of 12.7cm was assumed when calculating forces consistent with the actual size of the plate in the present experimental study. The main surfaces of the plate were set to 410K (cold) and 450K (hot), and the sidewalls were 430K. The chamber wall temperature was assumed to be constant at 300K. The computations were performed for chamber pressures ranging 0.006Pa to 6Pa and chamber sizes from 0.45cm to 1.8m using three gases: helium, nitrogen, and argon. For the solution of the ES model equation, argon and helium were considered with the same flow conditions as in DSMC. Three-blocks, non-uniform rectangular grid was used in the solution of the ES equation with the total of 13,359 spatial nodes. The Gauss-Hermite quadrature of order 16 and three-eighths rule were used for discretization of velocity magnitude and angle, respectively.

RESULTS

The pressure field inside the chamber for both free molecule and near continuum conditions are shown in Fig. 2, where the ratios of the local pressure over the free stream value are presented for helium at a chamber pressure of both .006Pa (top) and 6Pa(bottom). The computation domain of 0.45x0.45m is bounded by 300K diffuse walls, and the hot side of the radiometer is on the left hand side of the plate. The highest over-pressure occurs in the regions nearest the hot face in both of the plots, and the difference between the hot and cold sides is decidedly larger under low-pressure conditions.

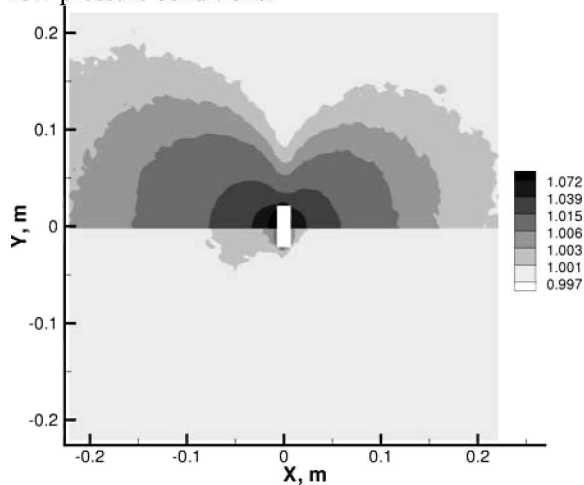


FIGURE 2. P/P_{inf} for two pressures, $P=0.006$ Pa (top) and $P=6$ Pa(bottom) in He.

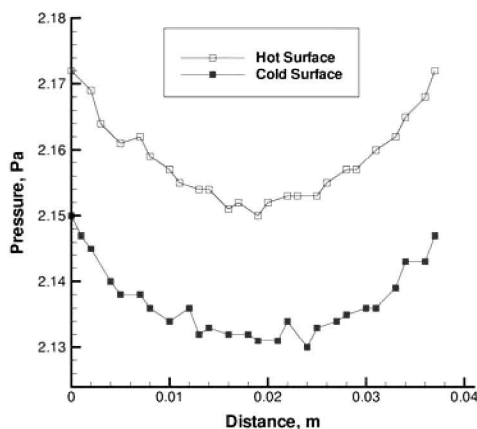


FIGURE 3. Pressure on main surfaces of the radiometer.

To examine the contribution of the edge effects to the net force, and analyze the relative importance of the forces on the edges of plate versus the area forces, the DSMC computations were performed in helium, for a geometric configuration of a 3.9cm tall plate. The surface pressure distribution over the cold and hot sides of the solid plate is shown in Fig. 3 for a chamber pressure of 2Pa. The pressure has a minimum near the center of the plate both for the hot and cold sides. The values near the edges are visibly larger than that near the center. The net force, however, is produced by the difference of pressure forces on the hot and cold sides of the plate, and the contribution of area and perimeter forces may be compared analyzing the pressure difference near the center of the plate and closer to the edge.

The statistical scatter inherent in the DSMC method significantly complicates such an analysis, and the deterministic solution of the ES model kinetic equation was therefore used. Although it uses an approximation to the collision operator of the Boltzmann equation, the ES equation nevertheless is capable of capturing the main features of the radiometric flows. Comparison of the DSMC and ES solutions is presented in Fig. 4, where the temperature fields and streamlines are shown. The numerical results obtained by these two approaches are similar, and the difference in temperature is less than 1 percent. There are four vortices created by the temperature gradients, two at each side of the plate. The vortices at the hot side of the plate are noticeably stronger than at the cold side. For the case under consideration, the maximum flow speed in the hot surface vortices is about 5m/s, and in the cold surface vortices it is about 2m/s. Note that the vortex structure is similar to that calculated by Ota¹² but qualitatively differs from the flow structure given by Kennard.²²

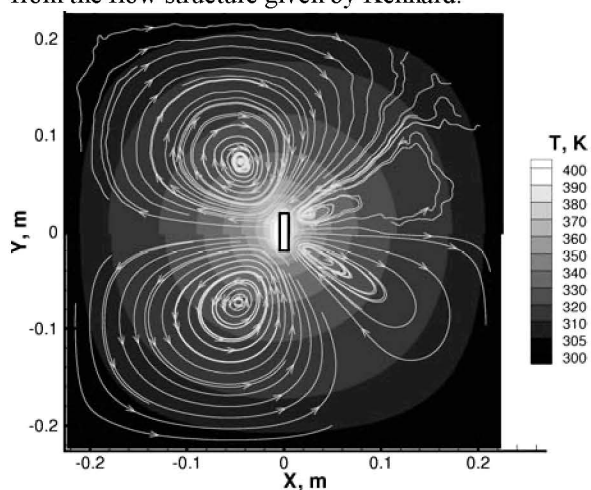


FIGURE 4. DSMC (top) and ES (bottom) solutions for He at 2Pa.

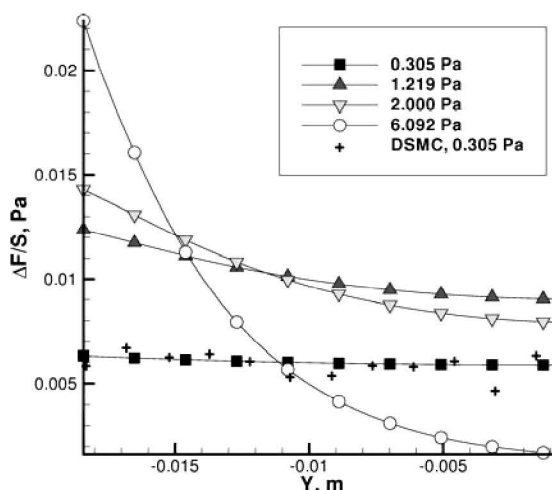


FIGURE 5. Pressure difference along the vane for Ar.

The pressure difference distribution along the vane (the difference between the force on the hot and cold sides divided by the surface area, S) is given in Fig. 5 for pure argon at four pressures. Note that the pressure of 1.219Pa corresponds to the maximum radiometric force. Only half of the plate is shown here, and the coordinate $Y=0$ corresponds to the center of the vane. For the lowest pressure shown in this figure, the pressure difference near the center is close to that near the edge, which indicates that the area force is the main contributor to the radiometric force. For the higher pressure, the opposite is true: the perimeter, or edge, force is the determining factor. Both area and perimeter forces are contributing for gas pressures corresponding to the maximum radiometric forces, with the area force appearing to be somewhat larger. Comparison with the DSMC results shows good agreement for the tested pressure.

Experimental results for nitrogen in the small chamber are shown in Fig. 6. It is readily observed in the low pressure region that the circular plate and large rectangular plate collapse onto each other and that their values are very close to twice that of the smaller plate. This is expected, as free molecular theory shows the force to be entirely dependent on area. As the flow transitions from the collisionless regime, the picture becomes less clear. While it is readily observed that the plates with larger area produce more force at their respective peaks, the force to area ratio does not hold.

When comparing the peaks of the large and small rectangles, it is found that the small plate creates 65% of the force of the larger one. Interestingly, this is almost precisely half way between the area ratio (50%) and the perimeter ratio (81%). Were that the only data presented, it would be tempting to presume that the perimeter force

was slowly beginning to dominate. This does not entirely appear to be the case however, as the peak force created by the circle is decidedly larger by approximately 7%. It seems quite contradictory that a device with 14% less perimeter would create a larger force without an equivalent increase in heated surface. This increase in force is possibly explained by more efficient pressure redistribution in front of the plate due to the axial symmetry of the circular plate vortices.

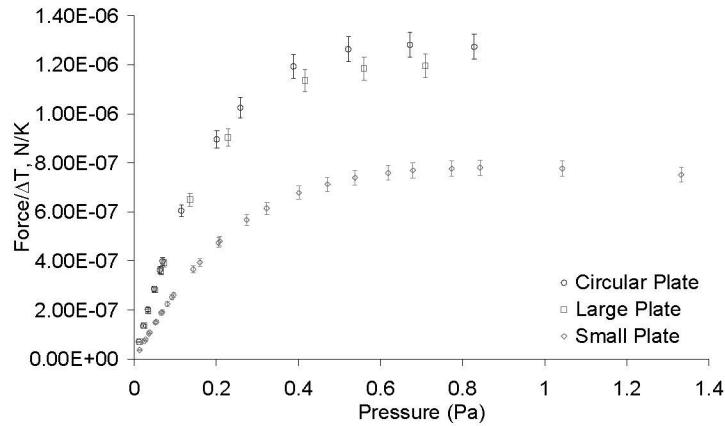


FIGURE 6. Normalized force for different device geometries in the 0.4m chamber.

The numerical predictions obtained for two different plate sizes are shown in Fig. 7 and are qualitatively similar to the above measurements. In the free molecular regime, the larger plate produces a proportionally larger force. The ratio of the small plate force to the large plate force increases with pressure and reaches about 0.7 in the range of pressures where the force is maximum. This further indicates that the area is still a large contributor to the peak force, where it must be noted that the perimeter ratio of the 2-D case is unity.

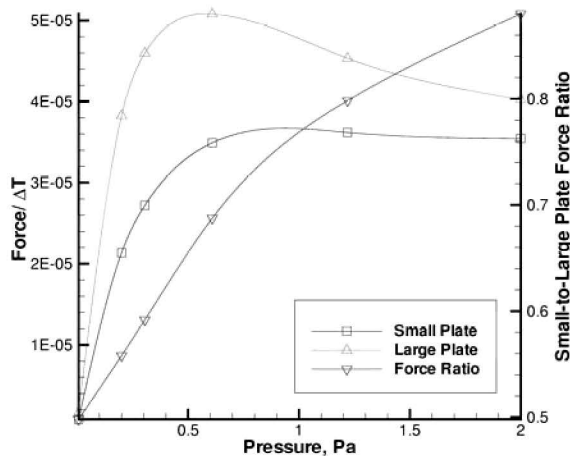


FIGURE 7. Numerical results for two different plates.

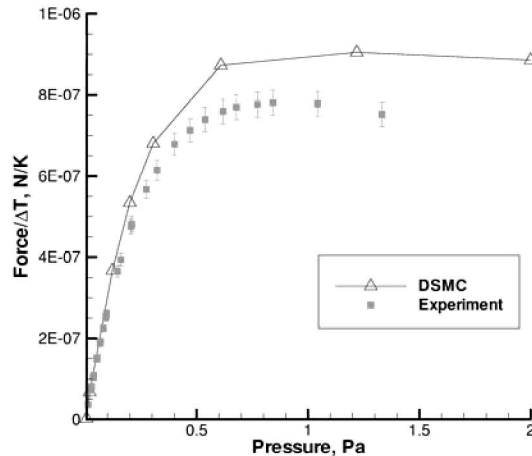


FIGURE 8. Comparison of experimental and computational results.

Comparison of the DSMC results and experimental measurements of the net force on the plate in nitrogen is shown in Fig. 8 for different pressures. The force is normalized by the temperature difference between the cold and hot surfaces, since the actual values of the temperature somewhat varied in the experiment. The comparison shows that both measurements and DSMC predict pressure maximum around 1 Pa. The numerical results noticeably over-predict the measurements, with the difference attributed primarily to the three dimensionality of the experiment and an incomplete energy accommodation that was not accounted for in DSMC.

CONCLUSION

A study of the radiometric forces on heated plates has been conducted both experimentally and computationally. The experiments were carried out in a 0.4m vacuum chamber up to a maximum pressure of 1.2 Pa for various carrier gases. The computations were performed with the DSMC method and a solution of the ES model kinetic equation for a 2-D gas flow over a comparable range of pressures. It is shown that the radiometric devices provide maximum force at a Knudsen number approximating 0.1. Qualitatively, the experimental data and computational results are similar. A lack of experimental data on gas-surface accommodation and flow three-dimensionality yields approximately a 25% difference in the magnitude of the measured and computed forces. Comparison of three geometric configurations has shown, both experimentally and numerically, that the effect of the area is significant at pressures up to where the force is maximum.

ACKNOWLEDGMENTS

The work at USC was supported in part by the Propulsion Directorate of the Air Force Research Laboratory at Edwards Air Force Base, California. The work at ERC was supported by the Air Force Office of Scientific Research. The authors thank Dr. Ingrid Wysong for many fruitful discussions.

REFERENCES

1. W. Crookes, "On attraction and repulsion resulting from radiation," *Phil. Trans. R. Soc.*, **163**, 277 (1873).
2. W. Crookes, "On attraction and repulsion resulting from radiation," *Phil. Trans. R. Soc.*, **165**, 519 (1875).
3. O. Reynolds, "On the forces caused by the communication of heat between a surface and a gas; and on a new photometer," *Phil. Trans. R. Soc.*, **166**, 725 (1876).
4. A. Schuster, *Phil. Trans. R. Soc.*, **166**, 715 (1876).
5. O. Reynolds, *Phil. Trans. R. Soc.*, **170**, 727 (1879).
6. J.C. Maxwell, "On stresses in rarefied gases arising from inequalities of temperature," *Phil. Trans. R. Soc.*, **170**, 231 (1879).
7. A. Einstein, "Zur theorie der fadiometerkrafte," *Z. Physik*, **27**, 1 (1924).
8. H. E. Marsh, *J. Opt. Soc. Amer.*, **12**, 135 (1926).
9. C. W. Draper, "The Crookes radiometer revisited," *J. Chem. Education*, **53**(6), 357 (1976).
10. E. A. Mason, B. Block, "Molecular inelastic collision cross sections from the radiometer force," *Annals of Physics*, **1**, 7 (1966).
11. D.C. Wadsworth, E.P. Muntz, "A computational study of radiometric phenomena for powering microactuators with unlimited displacements and large available forces," *J. Microelectromech. Syst.*, **5**(1), 59.
12. M. Ota, T. Nakao, M. Sakamoto, "Numerical simulation of molecular motion around laser microengine blades," *Math. and Computers in Simulation*, **55**, 223 (2001).
13. A. Passian, A. Wig, F. Meriaudeau, T.L. Ferrell, T. Thundat, "Knudsen forces on microcantilevers," *J. Appl. Phys.*, **92**(10), 6326 (2002).
14. A. Passian, R. J. Warmack, A. Wig, et al., "Observation of Knudsen effects with microcantilevers," *Ultramicroscopy*, **97**, 401 (2003).
15. A. Passian, R. J. Warmack, T.L. Ferrell, T. Thundat, "Thermal transpiration at the microscale: a Crookes cantilever," *Phys. Rev. Letters*, **90**(12), 124503 (2003).
16. G. Benford, J. Benford, "An aero-spacecraft for the upper atmosphere supported by microwaves," *Acta Austonautica*, **56**, 529 (2005).
17. A.J. Jamison, A.D. Ketsdever, and E.P. Muntz, "Gas dynamic calibration of a nano-Newton thrust stand," *Review of Scientific Instruments*, **73**, 3629 (2002).
18. N.P. Selden, A.D. Ketsdever, "Comparison of force balance calibration techniques for the nano-Newton range," *Review of Scientific Instruments*, **74**, 5249 (2003).
19. N. Selden, C. Ngalande, S. Gimelshein, and A. Ketsdever, "Experimental and Computational Observation of Radiometric Force on a Plate," *AIAA Thermophysics Conference*, June 2007.
20. M.S. Ivanov, G.N. Markelov, S.F. Gimelshein, "Statistical simulation of reactive rarefied flows: numerical approach and applications," *AIAA Paper 98-2669* (1998).
21. Bird, G.A., *Molecular Gas Dynamics and the Direct Simulation of Gas Flows*, Clarendon Press, Oxford (1994).
22. E.H. Kennard, "Kinetic Theory of Gases," McGraw-Hill Inc., New York (1938).